Mechanism and Machine Theory 182 (2023) 105222

Contents lists available at ScienceDirect

Mechanism and Machine Theory

journal homepage: www.elsevier.com/locate/mechmt

Research paper

Planar and spherical four-bar linkage $v_i - v_j$ algebraic input–output equations

M. John D. Hayes *, Mirja Rotzoll, Quinn Bucciol, Zachary A. Copeland

Carleton University, 1125 Colonel By Drive, Ottawa, ON, K1S 5B6, Canada

ARTICLE INFO

Keywords:
Planar and spherical four-bar linkages
v_i–v_j algebraic input–output equations
Algebraic polynomial elimination methods

ABSTRACT

The algebraic polynomial input–output (IO) equations relating any two of the relative joint displacement parameters, called v_i and v_j, between any of the six distinct pairs of rigid links in arbitrary planar and spherical four-bar mechanisms are derived. First, the forward kinematics transformation matrices of the corresponding serial kinematic chains are computed in terms of their Denavit–Hartenberg parameters, but with all angles converted to tangent half-angle parameters. These matrices are mapped to their corresponding Study soma coordinates. The serial kinematic chain is closed by equating the soma coordinates to the identity array. Algebraic polynomial elimination methods are then used to obtain a single polynomial in terms of only the design and the selected IO joint displacement parameters. This yields six independent algebraic IO Equations for each of the planar and spherical 4R linkages; the same techniques are applied to derive six additional algebraic IO equations for each of the RRRP and PRRP planar linkages providing a catalogue of 24. The utility of these IO equation sets is demonstrated via discussion of the associated mobility and design parameter spaces.

1. Introduction

Relative motion between mechanically constrained rigid bodies in the plane, on the surface of a sphere, and in three-dimensional space has fascinated philosophers, mathematicians, and engineers for millennia [1]. The design of predictable motion of a four-bar spherical mechanism appears to have its origins in the development of universal joints based on gimbals, which have also been investigated since antiquity [2]. While there is a substantial volume of archival literature regarding planar and spherical 4R mechanisms, see [3–7] for a small but relevant sample, these types of mechanical systems still excite the imagination, see [8–12] for recent examples.

Eduard Study, 1868–1930, likely inspired by the earlier work of Julius Plücker, 1801–1868, and his Ph.D. student Felix Klein, 1845–1925, on the development of line geometry [13–15], proposed the theory of mapping the special Euclidean group of rigid body displacements, $SE(3)$, to the points on a six-dimensional hyper-quadric in a seven-dimensional projective space, now known as the Study quadric S_6^2 [16]. The relative displacements of rigid bodies in a plane and on the surface of a sphere map to subspaces of S_6^2. Study called the coordinates of points of this space soma, the Greek word for body. These soma coordinates lead to algebraic polynomials in terms of the joint variables and design parameters for the relative displacements of any particular mechanical system. Study's kinematic mapping image space was notably reintroduced to the research world in [17,18], and will be relied upon in this paper.

All moveable four-bar linkages generate six distinct functions between the four distinct joint variable parameters taken two at a time, which we abstractly call v_i and v_j. While this is common knowledge in the kinematics community, there do not exist

* Corresponding author.
E-mail address: john.hayes@carleton.ca (M.J.D. Hayes).

https://doi.org/10.1016/j.mechmachtheory.2022.105222
Received 25 October 2022; Received in revised form 11 December 2022; Accepted 25 December 2022

Table 1
DH parameters for an arbitrary open 4R chain.

Axis i	Link length a_i	Angle θ_i	Link offset d_i	Twist τ_i
1	a_1	θ_1	0	0
2	a_2	θ_2	0	0
3	a_3	θ_3	0	0
4	a_4	θ_4	0	0

convenient and consistent ways to determine and express these six functions using algebraic means. Moreover, only the $v_1 - v_4$ and $v_1 - v_3$ IO equations can be found in vast body of archival literature, but they are expressed as trigonometric implicit equations, see [3,8] for standard examples. Hence, we believe this is sufficient justification to present the work on the derivation of the six $v_i - v_j$ algebraic input–output (IO) equations for each of the planar 4R, RRRP, PRRP, and spherical 4R linkages reported herein. The motivation at the foundation of this work is to provide computational tools for mechanism design and analysis that are less cumbersome to use than vector loop methods based on trigonometry. Since our IO equations are algebraic polynomials of degree 4, and 3 or 2 for the PRRP, in two variables with rational coefficients, the full power of the theory of planar algebraic curves [19] can be applied to these 24 distinct algebraic IO curves in their respective $v_i - v_j$ parameter planes. This enables one to observe significantly more and comparatively simple to obtain information regarding all the relative motions generated by the linkage.

In this paper we present a novel algorithm, built on tools from algebraic-geometry, that derives the algebraic polynomials which model the relative displacements of all six IO joint displacement pairs in each class of arbitrary planar and spherical single degree of freedom simple closed kinematic chains. First, the class of open kinematic chains is parameterised using the well known notation for lower-pair kinematic chains of arbitrary architecture: Denavit–Hartenberg (DH) notation [4]. The resulting coordinate transformation matrix describing the forward kinematics of the open chain is equated to the identity matrix to conceptually close the chain [4]. Measures of angle elements in the resulting matrix are converted to their respective tangent half-angle parameters. This modified transformation matrix is then mapped to the coordinates of the seven dimensional projective kinematic image space using the well known definitions of the Study soma coordinates [16,17,20,21]. Next, using an appropriate subset of the soma, elimination theory [22] is used to eliminate undesired variable joint displacement parameters leaving only the implicit algebraic IO equation for the desired IO parameter pair. The first presentation of a part of the algorithm can be found in [23]. However, in that work we failed to understand how completely general the algorithm is and this work will provide the generalisation. While we have already successfully applied the algorithm to derive the algebraic IO equations for some planar and spherical four-bar linkages [24], here we will derive the six different $v_i - v_j$ IO equations for each of the planar 4R, RRRP, PRRP and spherical 4R linkages, and thereby provide a long needed catalogue of these 24 algebraic IO equations.

2. Planar four-bar linkages

We start with a generic 4R open kinematic chain and assign the standard DH coordinate systems and parameters according to [4], see Table 1 and Fig. 1(a). The four link lengths are the a_i, and the four joint angles are the θ_i, $i \in \{1, 2, 3, 4\}$. While we do not require them for the planar 4R, there are non-zero link twist angles, τ_i, for the RRRP, PRRP, and spherical 4R linkages, as well as link offsets, d_i, for the RRRP and PRRP linkages. All measures of angle are converted to algebraic parameters using the tangent half-angle substitutions:

$$v_i = \tan\frac{\theta_i}{2} \quad \Rightarrow \quad \cos\theta_i = \frac{1 - v_i^2}{1 + v_i^2}, \quad \sin\theta_i = \frac{2v_i}{1 + v_i^2},$$

$$\alpha_i = \tan\frac{\tau_i}{2} \quad \Rightarrow \quad \cos\tau_i = \frac{1 - \alpha_i^2}{1 + \alpha_i^2}, \quad \sin\tau_i = \frac{2\alpha_i}{1 + \alpha_i^2}.$$

The transformation matrix implied by the algebrised parameters is equated to the identity matrix thereby conceptually closing the kinematic chain. Closing the serial 4R chain by grounding link a_4 means that we may have clockwise (CW) or counter clockwise (CCW) joint index circulation. The CW circulation means that the origins of $x_4 - y_4$ and $x_0 - y_0$ are coincident, but the basis vector directions in each coordinate system are out of phase by π radians. Whereas the CCW circulation means the two coordinate systems are congruent, see Fig. 1(b), and we call them the $x_{0/4}$ - $y_{0/4}$ coordinate system. The equations that follow are expressed in that coordinate system.

Using the definitions found in [23], the DH transformation matrix of the open 4R chain is mapped to the soma array of eight homogeneous coordinates

$$[x_0 : x_1 : x_2 : x_3 : y_0 : y_1 : y_2 : y_3].$$

Since we are only considering the special Euclidean subgroup of direct planar isometries $SE(2)$ generated by planar 4R, RRRP, and PRRP linkages at the moment, four of the soma coordinates always vanish and what remains are

$$\text{planar 4R and RRRP: } [x_0 : 0 : 0 : x_3 : 0 : y_1 : y_2 : 0]; \tag{1}$$

$$\text{PRRP: } [x_0 : x_1 : 0 : 0 : 0 : 0 : y_2 : y_3]. \tag{2}$$

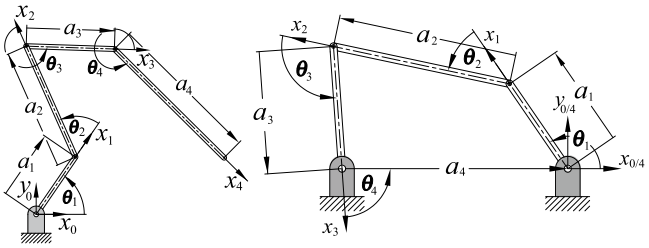

(a) Generic open 4R kinematic chain. (b) Generic closed 4R kinematic chain.

Fig. 1. Serial and parallel planar 4R linkages.

Regardless, for a generic representation we use the full Study array here since the 0 elements are also different for spherical linkages [23,25]. To close the planar serial 4R kinematic chain, the Study array is equated to the identity array thus

$$[x_0 : 0 : 0 : x_3 : 0 : y_1 : y_2 : 0] = [1 : 0 : 0 : 0 : 0 : 0 : 0 : 0]. \tag{3}$$

The Gröbner bases of the ideal generated by the three polynomials $x_3 = 0$, $y_1 = 0$, and $y_2 = 0$ are used to eliminate the two unwanted v_i joint angle parameters leading to the desired $v_i - v_j$ algebraic IO equation. For example, v_2 and v_4 must be eliminated to obtain the $v_1 - v_3$ algebraic IO equation. Because the soma are homogeneous coordinates, and because we are only interested in the kinematic images of real rigid body displacements, we will not use the homogenising coordinate $x_0 = 1$ as a polynomial in our elimination computations.

It is important to note that the IO equations may also be obtained directly on S_6^2. In [26] the DH transformations are expressed as 8×8 matrices and manipulated directly on S_6^2. When equated to the identity array, the IO equation can be obtained with elimination methods. Similarly, in [27] dual quaternions are used to obtain the closure equation of spatial 6R linkages. These methods could be applied to determine the soma coordinates, but that is not the focus of this paper. What is important is the general unified way to model the kinematic geometry of each of the four classes of four-bar linkage and obtain the six $v_i - v_j$ algebraic IO equations from the associated soma coordinates for each of the planar 4R, RRRP, PRRP, and spherical 4R linkages.

2.1. Derivation of the six planar 4R linkage $v_i - v_j$ IO equations

Let the input angle parameter be v_1 and the output angle parameter be v_4. In [23] two elimination steps were applied to the Gröbner bases of the ideal generated by the soma coordinates x_3, y_1 and y_2 to eliminate the angle parameters v_2 and v_3 from the equations yielding the algebraic IO equation relating the v_1 and v_4 angle parameters, which we call the $v_1 - v_4$ IO equation. It has the form

$$Av_1^2v_4^2 + Bv_1^2 + Cv_4^2 - 8a_1a_3v_1v_4 + D = 0, \tag{4}$$

where

$$\begin{aligned}
A &= A_1A_2 = (a_1 - a_2 + a_3 - a_4)(a_1 + a_2 + a_3 - a_4),\\
B &= B_1B_2 = (a_1 + a_2 - a_3 - a_4)(a_1 - a_2 - a_3 - a_4),\\
C &= C_1C_2 = (a_1 - a_2 - a_3 + a_4)(a_1 + a_2 - a_3 + a_4),\\
D &= D_1D_2 = (a_1 + a_2 + a_3 + a_4)(a_1 - a_2 + a_3 + a_4),\\
v_1 &= \tan\frac{\theta_1}{2},\\
v_4 &= \tan\frac{\theta_4}{2}.
\end{aligned}$$

This algebraic equation is of degree 4 in the v_1 and v_4 variable parameters, while the coefficients labelled A, B, C, and D are each products of two bilinear factors which can be viewed as eight distinct planes treating the four a_i link lengths as homogeneous coordinates. See Section 5.2 for a detailed description of this design parameter space.

In the approach used in [23] to obtain this IO equation from the ideal $\langle x_3, y_1, y_2\rangle$ both v_2 and v_3 are eliminated by first computing the Gröbner bases of the ideal using the Maple 2021 "`tdeg`" monomial ordering with the list sequence (v_3, v_2, v_4, v_1). This is *graded reverse lexicographic order*, also known as *degrevlex* in the literature [28], with indeterminate ordering $v_3 > v_2 > v_4 > v_1$. This monomial ordering sorts the terms by total degree before breaking ties between terms with identical degree by comparing the smallest indeterminate first and considering a higher degree as smaller in the term ordering. The execution of this step is immediate on a standard computer with an Intel Core i7-7700 CPU @ 3.60 GHz. In this case, 12 bases are computed, all functions of all four v_i. We eliminate v_2 and v_3 by computing the bases of these 12 with the reverse monomial ordering by using "`plex`", which is the *pure lexicographic order*, also known as *lex* [28]. This results in 8 new bases, with one that is a function of only v_1 and v_4 and the four a_i, which represents the IO equation we are looking for.

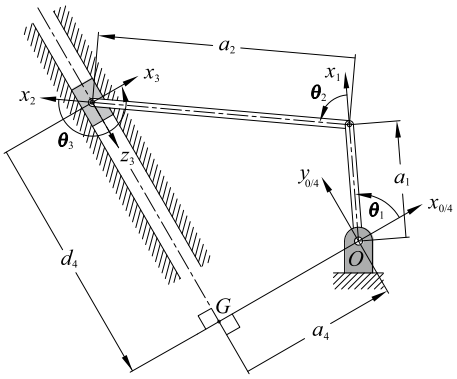

Fig. 2. Planar RRRP linkage with Denavit–Hartenberg coordinate system and parameter assignments.

However, we have since discovered that a single application of the elimination monomial ordering called "`lexdeg`" in Maple 2021 leads directly to the desired planar 4R $v_1 - v_4$ IO equation. When the ideal generated by the system of polynomials contains coefficients that are not too large or complicated, as for the planar 4R linkages, this elimination monomial ordering is very efficient, in the sense that it does not compute an entire "`plex`" basis. For the two disjoint lists of variables, those to be eliminated and those to be retained, the "`lexdeg`" ordering is equivalent to a product order which uses "`tdeg`" on each of the two disjoint lists of variables. All six of the distinct IO equations for each of the planar 4R, RRRP, and PRRP kinematic architectures are easily computed using the "`lexdeg`" elimination monomial ordering. This is how the IO equations for these planar four-bar linkages have been derived. For the planar 4R, the five remaining $v_i - v_j$ IO equations each contain all eight of the bilinear factors of the coefficients labelled $A_1, A_2, B_1, B_2, C_1, C_2, D_1$, and D_2 in Eq. (4), but in different permutations. This means that the design parameter space, as defined in [29], is the same for all six of these IO equations. The execution of the code is immediate for all six IO equations for each of the three kinematic architectures.

By applying the "`lexdeg`" monomial term orderings to the planar 4R variables in the appropriate disjoint lists, the $v_1 - v_2$, $v_1 - v_3$, $v_2 - v_3$, $v_2 - v_4$, and $v_3 - v_4$ IO equations are obtained and listed as follows.

$$A_1B_2v_1^2v_2^2 + A_2B_1v_1^2 + C_1D_2v_2^2 - 8a_2a_4v_1v_2 + C_2D_1 = 0, \tag{5}$$

$$A_1B_1v_1^2v_3^2 + A_2B_2v_1^2 + C_2D_2v_3^2 + C_1D_1 = 0, \tag{6}$$

$$A_1D_2v_2^2v_3^2 + B_2C_1v_2^2 + B_1C_2v_3^2 - 8a_1a_3v_2v_3 + A_2D_1 = 0, \tag{7}$$

$$A_1C_1v_2^2v_4^2 + B_2D_2v_2^2 + A_2C_2v_4^2 + B_1D_1 = 0, \tag{8}$$

$$A_1C_2v_3^2v_4^2 + B_1D_2v_3^2 + A_2C_1v_4^2 + 8a_2a_4v_3v_4 + B_2D_1 = 0. \tag{9}$$

Eqs. (4), (5), (7), and (9) all contain a bilinear quadratic term because they relate adjacent angle pairs, while Eqs. (6) and (8) relate opposite angle pairs, and hence do not possess a bilinear quadratic term.

Each of these six IO equations is of degree 4 in the two variable angle parameters, defining quartic curves in the planes spanned by the different $v_i - v_j$ angle parameter pairs. They also all have genus 1 meaning that there is a maximum number of two assembly modes. This is so because of a theorem on algebraic curves proved by Axel Harnack in 1876 [30] which relates the circuits of an algebraic curve to its genus. Each of the $v_i - v_j$ algebraic IO equations are quartic curves of genus 1, therefore, following Harnack, each can have at most two circuits. Each circuit of a particular $v_i - v_j$ IO curve corresponds to one of the mechanisms assembly modes. In essence, Harnack's theorem states that an algebraic curve of genus n can have at most $n + 1$ circuits. One may therefore immediately conclude that a planar 4R mechanism can never have more than two assembly modes.

2.2. Six planar RRRP linkage $v_i - v_j$ IO equations

Next we shall list the six algebraic IO equations for planar RRRP mechanisms obtained using our technique employing the "`lexdeg`" elimination monomial ordering. An arbitrary RRRP linkage is illustrated in Fig. 2. The P-pair z_3-axis induces the two link twist angles and a link offset listed in Table 2.

Applying the methods in [23] to the DH parameters by algebraising the angle parameters with tangent half-angle equivalents, projecting the DH closure equation into Study's kinematic mapping image space as soma coordinates, then eliminating the intermediate joint variable parameters v_2 and v_3 using "`lexdeg`" leads to the RRRP $v_1 - d_4$ algebraic IO equation:

$$v_1^2d_4^2 + Rv_1^2 + d_4^2 - 4a_1v_1d_4 + S = 0, \tag{10}$$

where

$$R = R_1R_2 = (a_1 + a_2 - a_4)(a_1 - a_2 - a_4),$$

Table 2
DH parameters for the RRRP.

i	θ_i	d_i	a_i	τ_i	α_i
1	θ_1	0	a_1	0	0
2	θ_2	0	a_2	0	0
3	θ_3	0	0	$\pi/2$	1
4	0	d_4	a_4	$-\pi/2$	-1

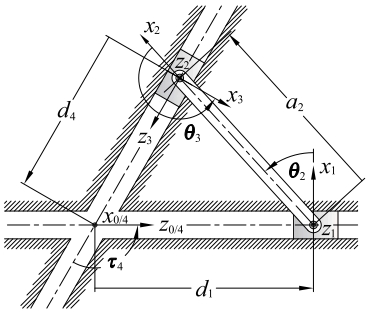

Fig. 3. Planar PRRP linkage with Denavit–Hartenberg coordinate systems and parameter assignments.

Table 3
DH parameters for the PRRP.

i	θ_i	v_i	d_i	a_i	τ_i	α_i
1	$-\pi/2$	-1	d_1	0	$-\pi/2$	-1
2	θ_2	v_2	0	a_2	0	0
3	θ_3	v_2	0	0	$\pi/2$	1
4	$\pi/2$	1	d_4	0	τ_4	α_4

$$S = S_1 S_2 = (a_1 + a_2 + a_4)(a_1 - a_2 + a_4),$$
$$v_1 = \tan\frac{\theta_1}{2}.$$

The four bilinear factors R_1, R_2, S_1, and S_2 can be regarded as four planes intersecting in the faces of a four-sided pyramid in the design parameter space orthogonally spanned by the three lengths a_1, a_2, and a_4, see [31] for a detailed description.

Using the same approach, the five remaining joint variable parameter pairings lead to the following five additional RRRP algebraic IO equations:

$$R_2 v_1^2 v_2^2 + R_1 v_1^2 - S_2 v_2^2 + 4a_2 v_1 v_2 - S_1 = 0; \tag{11}$$
$$R_1 v_1^2 v_3^2 + R_2 v_1^2 - S_2 v_3^2 - S_1 = 0; \tag{12}$$
$$S_2 v_2^2 v_3^2 - R_2 v_2^2 - R_1 v_3^2 - 4a_1 v_2 v_3 + S_1 = 0; \tag{13}$$
$$v_2^2 d_4^2 - R_2 S_2 v_2^2 + d_4^2 - R_1 S_1 = 0; \tag{14}$$
$$v_3^2 d_4^2 - R_1 S_2 v_3^2 + d_4^2 + 4a_2 v_3 d_4 - R_2 S_1 = 0. \tag{15}$$

All six of the RRRP algebraic IO equations are of degree 4, representing quartic curves in the respective joint variable parameter planes. These six IO equations also all possess genus 1 meaning again that there is a maximum number of two assembly modes.

For the RRRP linkages that are rocker-sliders, each distinct circuit of the IO curve also contains two branches, one for each working mode. When the input angle reaches minimum or maximum values the mechanism instantaneously stops moving as the coupler becomes perpendicular to the direction of travel of the P-pair. In this singular configuration, unless mechanical constraints are imposed, the slider may move in one of two directions as the rocker input link begins to move again in the opposite sense. These are defined as the working modes of the particular assembly mode. Each working mode traces a distinct branch in the particular circuit of the IO curve. Together, both branches cover the entire circuit.

2.3. Six planar PRRP linkage $v_i - v_j$ IO equations

An identical approach is used for the planar PRRP linkages. Referring to Fig. 3, it is to be seen that general PRRP elliptical trammel linkages have but two design parameters, namely a_2 and τ_4, the coupler length, and the twist angle between the two P-pairs. The twist angle is typically $\tau_4 = \pi/2$, though it can be any other value. The DH parameters for an arbitrary PRRP are listed in Table 3. Again we apply the methods in [23] and the "`lexdeg`" monomial ordering to the DH parameters of the PRRP by algebraising the

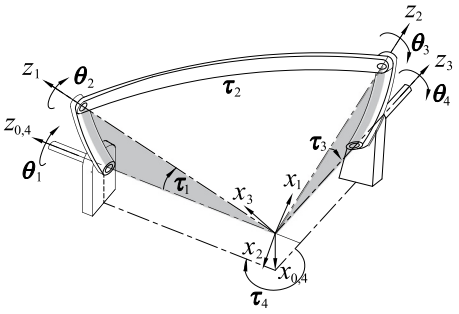

Fig. 4. Spherical 4R DH reference frames and parameters.

angle parameters with tangent half-angle equivalents, projecting the DH closure equation into Study's kinematic mapping image space as soma coordinates, then eliminating the intermediate joint variable parameters leading to the PRRP algebraic IO equations. The symmetry of the six algebraic IO equations is clearly revealed when we define the following three coefficients:

$$\begin{aligned} T &= a_2^2(\alpha_4^2+1);\\ U &= a_2(\alpha_4^2-1);\\ V &= a_2(\alpha_4^2+1). \end{aligned}$$

Using these coefficients the six algebraic IO equations are:

$$(\alpha_4^2+1)(d_1^2+d_4^2)-2(\alpha_4^2-1)d_1d_4-T=0; \tag{16}$$

$$2\alpha_4 d_1 v_2^2+Uv_2^2+2\alpha_4 d_1-4a_2\alpha_4 v_2-U=0; \tag{17}$$

$$2\alpha_4 d_1 v_3^2-Vv_3^2+2\alpha_4 d_1+V=0; \tag{18}$$

$$\alpha_4 v_2 v_3-v_2-v_3-\alpha_4=0; \tag{19}$$

$$2\alpha_4 v_2^2 d_4+Vv_2^2+2\alpha_4 d_4-V=0; \tag{20}$$

$$2\alpha_4 v_3^2 d_4-Uv_3^2+4a_2\alpha_4 v_3+2\alpha_4 d_4+U=0. \tag{21}$$

It is to be seen that Eqs. (17), (18), (20), and (21) are of degree 3, representing cubic curves in their respective joint variable parameter planes, while Eqs. (16) and (19) are of degree 2, and are different conics. When the respective quadratic forms are diagonalised it is easy to show that Eq. (16) is an ellipse, while Eq. (19) is an hyperbola which depends only on the link twist α_4. Moreover, each of the six PRRP algebraic IO equations, Eqs. (16)–(21) possess genus 0, unlike the planar 4R and RRRP IO equations. According to Harnak's theorem we conclude that the PRRP linkage has at most one assembly mode since each IO equation has a single circuit.

3. Spherical 4R linkages

Consider the arbitrary spherical 4R linkage illustrated in Fig. 4. The general IO equation expresses the implicit functional relationship between the input and output angles, θ_i and θ_j, in terms of the constant twist angles between the four R-pair centres, τ_i. For a unit sphere, the twist angles are equivalent to the corresponding arc lengths. The derivation of the algebraic form of the spherical IO equation [23] also makes use of the original Denavit–Hartenberg (DH) parametrisation of the kinematic geometry [32].

The forward kinematics of an arbitrary serial 4R spherical kinematic chain is obtained as a linear transformation matrix in terms of the DH parameters. This linear transformation can then be mapped to the corresponding eight Study soma coordinates [23]. For spherical kinematic chains there are also only four homogeneous soma coordinates since the displacement group contains only rotations about a fixed point. The corresponding Study array is:

$$[x_0 : x_1 : x_2 : x_3 : 0 : 0 : 0 : 0]. \tag{22}$$

The ideal generated by the three non-trivial soma that equate to zero, namely x_1, x_2, and x_3 are used to derive the algebraic IO equations relating the six distinct edges of an arbitrary spherical quadrangle.

Algebrising the joint angles and link twists with the tangent half-angle parameters $v_i = \tan(\theta_i/2)$ and $\alpha_i = \tan(\tau_i/2)$ leads to the algebraic form of each $v_i - v_j$ IO equation. The $v_1 - v_4$ algebraic IO equation is

$$Av_1^2v_4^2+Bv_1^2+Cv_4^2+8\alpha_1\alpha_3\left(\alpha_4^2+1\right)\left(\alpha_2^2+1\right)v_1v_4+D=0, \tag{23}$$

where

$$A = A_1A_2 = \left(\alpha_1\alpha_2\alpha_3-\alpha_1\alpha_2\alpha_4+\alpha_1\alpha_3\alpha_4-\alpha_2\alpha_3\alpha_4+\alpha_1-\alpha_2+\alpha_3-\alpha_4\right)$$

$$
\begin{aligned}
 & \left(\alpha_1\alpha_2\alpha_3 - \alpha_1\alpha_2\alpha_4 - \alpha_1\alpha_3\alpha_4 - \alpha_2\alpha_3\alpha_4 - \alpha_1 - \alpha_2 - \alpha_3 + \alpha_4\right), \\
B \;=\; B_1B_2 \;=\; & \left(\alpha_1\alpha_2\alpha_3 + \alpha_1\alpha_2\alpha_4 - \alpha_1\alpha_3\alpha_4 - \alpha_2\alpha_3\alpha_4 + \alpha_1 + \alpha_2 - \alpha_3 - \alpha_4\right) \\
 & \left(\alpha_1\alpha_2\alpha_3 + \alpha_1\alpha_2\alpha_4 + \alpha_1\alpha_3\alpha_4 - \alpha_2\alpha_3\alpha_4 - \alpha_1 + \alpha_2 + \alpha_3 + \alpha_4\right), \\
C \;=\; C_1C_2 \;=\; & \left(\alpha_1\alpha_2\alpha_3 - \alpha_1\alpha_2\alpha_4 - \alpha_1\alpha_3\alpha_4 + \alpha_2\alpha_3\alpha_4 - \alpha_1 + \alpha_2 + \alpha_3 - \alpha_4\right) \\
 & \left(\alpha_1\alpha_2\alpha_3 - \alpha_1\alpha_2\alpha_4 + \alpha_1\alpha_3\alpha_4 + \alpha_2\alpha_3\alpha_4 + \alpha_1 + \alpha_2 - \alpha_3 + \alpha_4\right), \\
D \;=\; D_1D_2 \;=\; & \left(\alpha_1\alpha_2\alpha_3 + \alpha_1\alpha_2\alpha_4 + \alpha_1\alpha_3\alpha_4 + \alpha_2\alpha_3\alpha_4 - \alpha_1 - \alpha_2 - \alpha_3 - \alpha_4\right) \\
 & \left(\alpha_1\alpha_2\alpha_3 + \alpha_1\alpha_2\alpha_4 - \alpha_1\alpha_3\alpha_4 + \alpha_2\alpha_3\alpha_4 + \alpha_1 - \alpha_2 + \alpha_3 + \alpha_4\right).
\end{aligned}
$$

The coefficients A, B, C, and D all have two bicubic factors. It can be shown that when the radius of the sphere is infinite then Eqs. (23) and (4) are functionally identical [23], hence the same coefficient names A, B, C, and D are used. While the derivation of this algebraised $v_1 - v_4$ IO equation is novel and far from intuitive, the algebraic form of this fourth degree polynomial in the $v_1 - v_4$ IO angle parameters is not. The earliest derivations of similar equations representing manipulatable octahedra, identical in form, are due to Raoul Bricard in 1897 [33]. This fascinating similarity between movable octahedral and spherical linkage algebraic IO equations is not at all a coincidence, as will be illustrated in Section 5.2.

4. Derivation of the six spherical $v_i - v_j$ IO equations

Using the eight bicubic coefficient definitions from Eq. (23), the remaining five $v_i - v_j$ equations contain all eight of the bicubic coefficients, but in different permutations:

$$A_1B_2v_1^2v_2^2 + A_2B_1v_1^2 + C_1D_2v_2^2 + 8\alpha_2\alpha_4\left(\alpha_1^2+1\right)\left(\alpha_3^2+1\right)v_1v_2 + C_2D_1 = 0; \tag{24}$$

$$A_1B_1v_1^2v_3^2 + A_2B_2v_1^2 + C_2D_2v_3^2 + C_1D_1 = 0; \tag{25}$$

$$A_1D_2v_2^2v_3^2 + B_2C_1v_2^2 + B_1C_2v_3^2 - 8\alpha_1\alpha_3\left(\alpha_2^2+1\right)\left(\alpha_4^2+1\right)v_2v_3 + A_2D_1 = 0; \tag{26}$$

$$A_1C_1v_2^2v_4^2 + B_2D_2v_2^2 + A_2C_2v_4^2 + B_1D_1 = 0; \tag{27}$$

$$A_1C_2v_3^2v_4^2 + B_1D_2v_3^2 + A_2C_1v_4^2 + 8\alpha_2\alpha_4\left(\alpha_1^2+1\right)\left(\alpha_3^2+1\right)v_3v_4 + B_2D_1 = 0. \tag{28}$$

As for the planar 4R and RRRP linkage algebraic IO equations, we see that Eqs. (25) and (27) do not contain a bilinear quadratic term because they relate angle parings between the spherical quadrangle edges that intersect in opposite vertices. Each of Eqs. (23)–(28) has genus 1.

The $v_1 - v_4$ IO Equation. The soma coordinates representing the forward kinematics of the spherical 4R are polynomials containing coefficients are already to complicated to efficiently use the "`lexdeg`" elimination monomial ordering. To obtain this IO equation from the ideal generated by the three soma coordinates that equate to zero, both v_2 and v_3 are eliminated by first computing the Gröbner bases using the Maple 2021 "`tdeg`" monomial ordering with the list sequence (v_3, v_2, v_4, v_1), meaning that the indeterminate ordering is $v_3 > v_2 > v_4 > v_1$. In this case, 12 bases are computed, all functions of all four v_i. We eliminate v_2 and v_3 by computing the bases of these 12 with the reverse monomial ordering by using "`plex`". This results in 10 new bases, with one that is a function of only v_1 and v_4 and the four α_i, which represents the IO equation we are looking for. This polynomial splits into three factors. The first two are $(1+v_1^2)(1+v_4^2)$, a product that is always greater than zero, and can be safely factored out, leaving us with Eq. (23). This, and some of the other spherical 4R IO equations are computable in one application of the "`lexdeg`" elimination monomial ordering, but the computation time is more than an order of magnitude greater, about 3500 s, than the 120 s for the sequential application of "`tdeg`" and "`plex`" on an Intel Core i7-7700 CPU @ 3.60 GHz.

It is important to note that we are using the standard Denavit–Hartenberg [32] relative joint angle parameters, which are each a measure of the relative angle a link makes with the previous link in the kinematic chain. This fact enables us to derive the remaining five IO equations such that the same eight bicubic coefficient factors characterise all six IO equations. This is generally not the case when vector loop methods are used together with trigonometry, see [34] for a detailed example.

The $v_1 - v_2$ IO Equation. The derivation steps are precisely the same as for the $v_1 - v_4$ IO equation. Eliminating v_3 and v_4 from the same three soma coordinates, the resulting $v_1 - v_2$ IO equation splits into three similar factors. The first two, $(1+v_1^2)(1+v_2^2)$, can be safely factored out, leaving us with Eq. (24).

The $v_1 - v_3$ IO Equation. The derivation steps are precisely the same as for the previous two IO equations. But, after the elimination of v_2 and v_4 from the same three soma coordinates, the resulting $v_1 - v_3$ IO equation splits into five factors. The first two are $(1+v_1^2)(1+v_3^2)$, and can be safely factored out. The next two are

$$(\alpha_2^2\alpha_3^2 + 2\alpha_2\alpha_3 + 1)v_3^2 + \alpha_2^2\alpha_3^2 - 2\alpha_2\alpha_3 + 1, \tag{29}$$

$$(\alpha_2^2 - 2\alpha_2\alpha_3 + \alpha_3^2)v_3^2 + \alpha_2^2 + 2\alpha_2\alpha_3 + \alpha_3^2. \tag{30}$$

In order for either, or both, of Eqs. (29) or (30) to be identically zero the arc length parameters α_2 and α_3 must be complex. This means these two factors may also eliminated since we are only interested in real linkages, leaving us with Eq. (25).

The $v_2 - v_3$ IO Equation. To derive this IO equation using elimination methods on the three soma coordinates we have been using requires a very different approach. We were successful by first applying the graded reverse lexicographical order "`tdeg`" to the

three soma coordinates using the list sequence (v_1, v_4, v_2, v_3), then applying *graded lexicographic order* using "grlex" to the bases identified with "tdeg". After each computation we obtain 12 bases, all in terms of the four α_i and the four v_i, with the exception of one in the graded lexicographic order set of bases, which is in terms of the four α_i, but only v_1, v_2, and v_3, and is used in the elimination steps. Next, resultants are used to eliminate v_4 first, then v_1. We obtain a $v_2 - v_3$ IO equation that splits into nine factors.

The first five of these factors are simple to divide out since they are trivially non-zero: the first is -1; the other four are the squares of a single α_i added to a positive integer. The next three factors are functions of v_2 and v_3, but only α_1, α_2, and α_3:

$$(\alpha_1\alpha_2 - \alpha_1\alpha_3 + \alpha_2\alpha_3 + 1)^2 v_2^2 v_3^2 + (\alpha_1\alpha_2 + \alpha_1\alpha_3 - \alpha_2\alpha_3 + 1)^2 v_2^2 + 8\alpha_1\alpha_3(\alpha_2^2 + 1)v_2 v_3 + (\alpha_1\alpha_2 - \alpha_1\alpha_3 - \alpha_2\alpha_3 - 1)^2 v_3^2 + (\alpha_1\alpha_2 + \alpha_1\alpha_3 + \alpha_2\alpha_3 - 1)^2; \tag{31}$$

$$(\alpha_1\alpha_2\alpha_3 + \alpha_1 - \alpha_2 + \alpha_3)^2 v_2^2 v_3^2 + (\alpha_1\alpha_2\alpha_3 - \alpha_1 + \alpha_2 + \alpha_3)^2 v_2^2 - 8\alpha_1\alpha_3(\alpha_2^2 + 1)v_2 v_3 + (\alpha_1\alpha_2\alpha_3 + \alpha_1 + \alpha_2 - \alpha_3)^2 v_3^2 + (\alpha_1\alpha_2\alpha_3 - \alpha_1 - \alpha_2 - \alpha_3)^2; \tag{32}$$

$$\alpha_3(\alpha_1\alpha_2 + 1)(\alpha_1 - \alpha_2)v_2^2 + 2\alpha_1\alpha_3(\alpha_2^2 + 1)v_2 v_3 - \alpha_1(\alpha_2\alpha_3 + 1)(\alpha_2 - \alpha_3)v_3^2 + \alpha_2(\alpha_1 + \alpha_3)(\alpha_1\alpha_3 - 1). \tag{33}$$

In order for Eqs. (31), (32), and/or (33) to be identically zero the arc length parameters α_1, α_2, and/or α_3 must be complex numbers, so we may safely divide these three factors out, leaving only Eq. (26) as the desired IO equation.

The $v_2 - v_4$ IO Equation. The derivation steps for the $v_2 - v_4$ IO equation are the same as those for the $v_1 - v_4$, $v_1 - v_2$, and $v_1 - v_3$ IO equations. The second set of Gröbner bases computed using the pure lexicographic order with list sequence (v_3, v_1, v_2, v_4) lead to an IO equation that splits into five factors, the first two are trivial. The next two are

$$(\alpha_1^2\alpha_2^2 + 2\alpha_1\alpha_2 + 1)v_2^2 + \alpha_1^2\alpha_2^2 - 2\alpha_1\alpha_2 + 1, \tag{34}$$

$$(\alpha_1^2 - 2\alpha_1\alpha_2 + \alpha_2^2)v_2^2 + \alpha_1^2 + 2\alpha_1\alpha_2 + \alpha_2^2. \tag{35}$$

For either, or both of Eqs. (34) and (35) to equate to zero, it requires both α_1 and α_2 to be complex. We can therefore factor both of these out, leaving only the desired $v_2 - v_4$ IO, Eq. (27).

The $v_3 - v_4$ IO Equation. Finally, the derivation steps for the $v_3 - v_4$ IO equation are precisely the same as for the $v_2 - v_4$ IO equation. After the elimination of v_1 and v_2 from the same three soma coordinates, the resulting $v_3 - v_4$ IO equation splits into three factors. The first two are safely divided out, leaving us with Eq. (28).

5. Applications

5.1. Mobility classification

Treating each pair of $v_i - v_j$ to be coordinate axes in the plane spanned by the two, then each IO equation for a pair of joint angle parameters contains two double points at infinity[1], one on each of the v_i and v_j axes. The double points at infinity belonging to each of the four distinct v_i coordinate axes together with the type of points at $v_i = 0$ completely define the mobility limits, if they exist, between each $v_i - v_j$ angle parameter pair. For a planar algebraic curve to possess a double point, its degree must be $n > 3$. Hence, this analysis does not apply to PRRP linkages, but it does apply to the R-pairs in an RRRP linkage. The double point at infinity on the d_4 axis is always an acnode independent of the lengths of the links and offsets, which is reassuring as this means the travel of the prismatic slider is always finite. But, for R-pairs, the nature of the double points determine if extreme orientations exist that are implied by the v_i where the two corresponding links can align. Hence, the examination of these two points is sufficient to determine whether a particular joint enables a crank, a rocker, a π-rocker, or a 0-rocker relative link motion [35,36].

For example, let us determine the double points for the $v_1 - v_4$ IO curve for a planar 4R. First homogenise Eq. (4) using the homogenising coordinate v_0, then redefine the IO equation as

$$k := Av_1^2v_4^2 + Bv_0^2v_1^2 + Cv_0^2v_4^2 - 8a_1a_3v_0^2v_1v_4 + Dv_0^4 = 0. \tag{36}$$

Then compute the partial derivatives of k with respect to the three homogeneous coordinates, giving

$$\frac{\partial k}{\partial v_0} := 2Bv_0v_1^2 + 2Cv_0v_4^2 - 16a_1a_3v_0v_1v_4 + 4Dv_0^3 = 0, \tag{37}$$

$$\frac{\partial k}{\partial v_1} := 2Av_1v_4^2 + 2Bv_0^2v_1 - 8a_1a_3v_0^2v_4 = 0, \tag{38}$$

$$\frac{\partial k}{\partial v_4} := 2Av_1^2v_4 + 2Cv_0^2v_4 - 8a_1a_3v_0^2v_1 = 0. \tag{39}$$

[1] The maximum number of double points for a planar algebraic curve of degree n is $\frac{(n-1)(n-2)}{2}$.

Finally solve the system of four Eqs. (36)–(39) for v_0, v_1, and v_4. In this case, similar for all the IO equations, there are two solutions which are independent of the design parameters a_1, a_2, a_3, and a_4. These two solutions are double points at infinity on the v_1 and v_4 axes, named DP_1 and DP_2:

$$DP_1 = \{v_0 = 0, v_1 = v_1, v_4 = 0\}; \tag{40}$$

$$DP_2 = \{v_0 = 0, v_1 = 0, v_4 = v_4\}. \tag{41}$$

One possibility to determine the type of double point, i.e., whether it is a crunode (regular double point), acnode (isolated double point), or cusp, is to evaluate whether the double point has a pair of real, or complex conjugate tangents. If the double point has two real distinct tangents, it is a crunode; if it has two real coincident tangents, it is a cusp; and if the tangents are both complex conjugates, the double point is an acnode [21,37]. Thus, after homogenising each $v_i - v_j$ angle pair IO equation using the homogenising coordinate v_0, leading to IO_h, the following discriminant yields information on the double point at infinity on the v_j axis:

$$\Delta := \left(\frac{\partial^2 IO_h}{\partial v_i \partial v_0}\right)^2 - \frac{\partial^2 IO_h}{\partial v_i^2}\frac{\partial^2 IO_h}{\partial v_0^2} \begin{cases} > & 0 & \Rightarrow & \text{crunode;} \\ = & 0 & \Rightarrow & \text{cusp;} \\ < & 0 & \Rightarrow & \text{acnode.} \end{cases} \tag{42}$$

Proceeding with the double point analysis of all six $v_i - v_j$ equations, the points at infinity on each axis result in 12 discriminants. However, as the $v_i - v_j$ equations are all dependent on each other, only four are distinct. Each one describes the nature of the double point at infinity of each v_i for $i \in \{1...4\}$:

$$\begin{aligned} \Delta_{v_1} = {} & -4(a_1 + a_2 - a_3 - a_4)(a_1 + a_2 + a_3 - a_4) \\ & (a_1 - a_2 + a_3 - a_4)(a_1 - a_2 - a_3 - a_4); \end{aligned}$$

$$\begin{aligned} \Delta_{v_2} = {} & -4(a_1 - a_2 - a_3 + a_4)(a_1 - a_2 + a_3 + a_4) \\ & (a_1 - a_2 + a_3 - a_4)(a_1 - a_2 - a_3 - a_4); \end{aligned}$$

$$\begin{aligned} \Delta_{v_3} = {} & -4(a_1 - a_2 + a_3 + a_4)(a_1 + a_2 - a_3 + a_4) \\ & (a_1 + a_2 - a_3 - a_4)(a_1 - a_2 + a_3 - a_4); \end{aligned}$$

$$\begin{aligned} \Delta_{v_4} = {} & -4(a_1 + a_2 - a_3 + a_4)(a_1 - a_2 - a_3 + a_4) \\ & (a_1 - a_2 + a_3 - a_4)(a_1 + a_2 + a_3 - a_4). \end{aligned}$$

Using the bilinear factors defined by Eq. (4) these discriminants can be rewritten compactly as

$$\Delta_{v_1} = -4\ A_1 A_2 B_1 B_2, \tag{43}$$

$$\Delta_{v_2} = -4\ A_1 B_2 C_1 D_2, \tag{44}$$

$$\Delta_{v_3} = -4\ A_1 B_1 C_2 D_2, \tag{45}$$

$$\Delta_{v_4} = -4\ A_1 A_2 C_1 C_2. \tag{46}$$

From these conditions we can extract the following information. If $\Delta_{v_1} \geq 0$, then the double point at infinity on the v_1 axis is either a crunode or a cusp. Knowing that $v_1 = \infty$ corresponds to $\theta_1 = 180°$, which implies that the link a_1 can physically reach the extreme position where a_1 aligns with and overlays the previous link a_4. Similarly, if $\Delta_{v_1} < 0$, then the double point at $v_1 = \infty$ is an acnode which in turn indicates that a_1 cannot physically reach the extreme position where a_1 aligns with and overlays a_4. Analogous conclusions can be drawn from Eqs. (44), (45), and (46).

As previously mentioned, to fully understand the mobility of every link, it equally requires the analysis of whether the other extremes where the link under investigation aligns with, but does not overlay, the previous link. We need to investigate whether the linkage is assemblable at $v_i = 0$. Clearly, one possibility to obtain a condition with this information can be derived using the six $v_i - v_j$ equations by substituting $v_i = 0$ and solving for v_j. Again, due to the equations' dependencies, we obtain four distinct conditions, one for each v_i:

$$\begin{aligned} \Omega_{v_1} = {} & [-(a_1 - a_2 - a_3 + a_4)(a_1 - a_2 + a_3 + a_4) \\ & (a_1 + a_2 - a_3 + a_4)(a_1 + a_2 + a_3 + a_4)]^{\frac{1}{2}}; \end{aligned}$$

$$\begin{aligned} \Omega_{v_2} = {} & [-(a_1 + a_2 - a_3 - a_4)(a_1 + a_2 + a_3 - a_4) \\ & (a_1 + a_2 - a_3 + a_4)(a_1 + a_2 + a_3 + a_4)]^{\frac{1}{2}}; \end{aligned}$$

$$\begin{aligned} \Omega_{v_3} = {} & [-(a_1 + a_2 + a_3 - a_4)(a_1 - a_2 - a_3 - a_4) \\ & (a_1 - a_2 - a_3 + a_4)(a_1 + a_2 + a_3 + a_4)]^{\frac{1}{2}}; \end{aligned}$$

Table 4
Mobility of a_1 relative to a_4.

$A_1A_2B_1B_2$	$C_1C_2D_1D_2$	Mobility of a_1
≤ 0	≤ 0	Crank
≤ 0	>0	π-rocker
>0	≤ 0	0-rocker
>0	>0	Rocker

Table 5
Mobility of a_2 relative to a_1.

$A_1B_2C_1D_2$	$A_2B_1C_2D_1$	Mobility of a_2
≤ 0	≤ 0	Crank
≤ 0	>0	π-rocker
>0	≤ 0	0-rocker
>0	>0	Rocker

Table 6
Mobility of a_3 relative to a_2.

$A_1B_1C_2D_2$	$A_2B_2C_1D_1$	Mobility of a_3
≤ 0	≤ 0	Crank
≤ 0	>0	π-rocker
>0	≤ 0	0-rocker
>0	>0	Rocker

Table 7
Mobility of a_4 relative to a_3.

$A_1A_2C_1C_2$	$B_1B_2D_1D_2$	Mobility of a_4
≤ 0	≤ 0	Crank
≤ 0	>0	π-rocker
>0	≤ 0	0-rocker
>0	>0	Rocker

$$\Omega_{v_4} = [-(a_1 - a_2 - a_3 - a_4)(a_1 + a_2 - a_3 - a_4)(a_1 - a_2 + a_3 + a_4)(a_1 + a_2 + a_3 + a_4)]^{\frac{1}{2}}.$$

Using the bilinear factors from Eq. (4) these expressions can be rewritten compactly as:

$$\Omega_{v_1} = \sqrt{-C_1C_2D_1D_2}; \tag{47}$$

$$\Omega_{v_2} = \sqrt{-A_2B_1C_2D_1}; \tag{48}$$

$$\Omega_{v_3} = \sqrt{-A_2B_2C_1D_1}; \tag{49}$$

$$\Omega_{v_4} = \sqrt{-B_1B_2D_1D_2}. \tag{50}$$

With this information we can establish a completely generic classification scheme to determine the relative mobilities of every link in the simple closed kinematic chain. Using the bilinear factors the classification can be constructed according to Tables 4–7. The beauty of this classification scheme lies in its completely generic nature, covering both positive and negative values for the a_i. This result requires the a_i to be considered as directed line segments. For example $a_1 > 0$ means that it is directed from the join with a_4 to a_2, $a_1 < 0$ means a_1 points in the opposite direction. Moreover, the classification scheme is directly linked to the algebraic IO equations. We are now able to explain the different spatial sections that are spanned by the linear factors in the design parameter space reported in [36].

It is straightforward to use this same analysis applied to the spherical 4R as well as the planar RRRP linkages to determine the relative mobility conditions for each link in the chain. However, in the interest if brevity, we will not include these results in this paper.

5.2. Design parameter spaces

The first graphical representation of the design parameter space of planar and spherical 4R linkages can be found in [38–40]. In the case of the planar 4R it reveals plane bound regions in a three-space having the Freudenstein parameters as mutually orthogonal basis vectors. However, the full symmetry of the group of planar 4R linkages is obscured by the trigonometric description of the IO

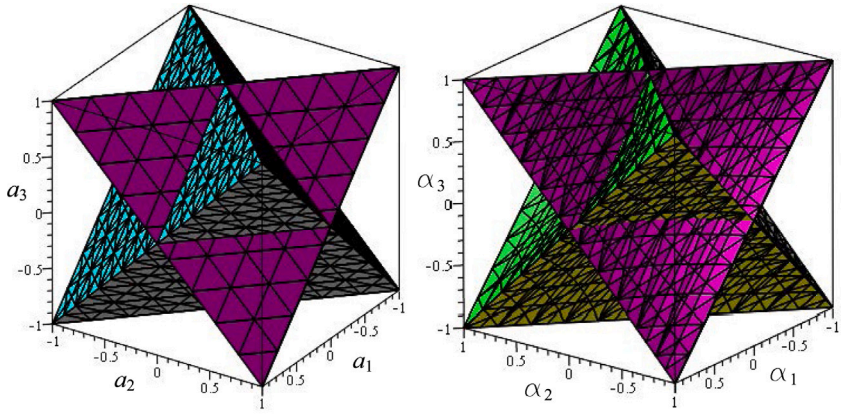

(a) Planar 4R stellated octahedron. (b) Spherical 4R degenerate bicubic surfaces.

Fig. 5. Planar and spherical 4R design parameter spaces.

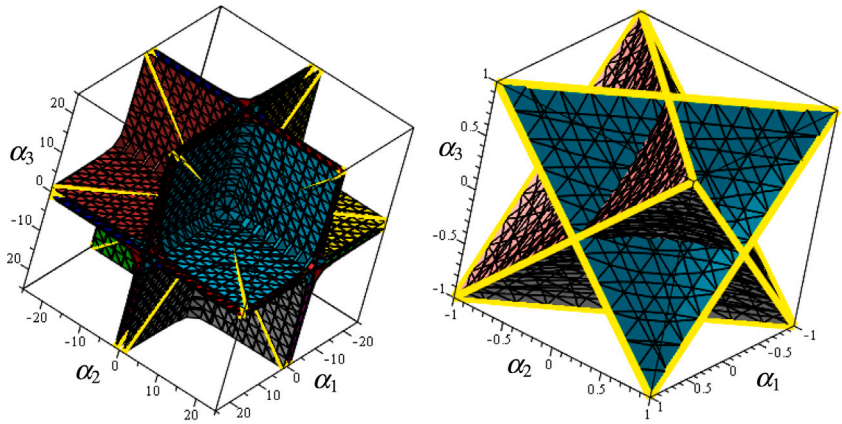

(a) In the range $-25 \leq \alpha_i \leq 25$. (b) In the range $-1 \leq \alpha_i \leq 1$.

Fig. 6. Eight cubic surfaces in the spherical 4R design parameter space.

equation. The symmetries of the algebraic IO equations for the spherical and planar 4R and the planar RRRP and PRRP linkages are fully revealed graphically when one considers the link lengths a_i, link offsets d_i, and link twist angle parameters α_i as design parameters, see [25,31,36]. For planar and spherical 4R function generators the scale of the linkage is irrelevant. We can consider these four a_i and four α_i design parameters as homogeneous coordinates, and assign a_4 and α_4 to normalise the four coordinates, thereby setting $a_4 = 1$ for the planar and $\alpha_4 = 1$ as the spherical design space parameter coordinates and treat the remaining three lengths or twist angles as mutually orthogonal basis vectors.

In the planar 4R design parameter three-space, each of the distinct eight bilinear factors in Eqs. (4)–(9) represent eight distinct planes. These eight planes intersect in 12 lines which are the edges of a setllated octahedron having order 48 octahedral symmetry [41], which Johannes Kepler named "stella octangula", which is Latin for "eight-pointed star", referring to the eight vertices, see Fig. 5(a). In the entire universe of polytopes, it is the only regular compound of two tetrahedra [41]: two tetrahedra which intersect in an octahedron! Each distinct point in the design parameter space represents a distinct planar 4R linkage. The eight planes segment the design parameter space into regions that represent the mobility of the linkages contained in that region [36,42].

For the spherical 4R, the eight bicubic factors in the four coefficients A, B, C, and D in Eq. (23) are symmetric singular cubic surfaces, see Fig. 5(b), which each possess three distinct finite lines and three common lines at infinity [25]. Note that a cubic surface can contain as many as 27 lines [43]; those that contain less than 27 are called *singular*, while those that contain exactly 27 are *non-singular*. Each of these cubic surfaces possess three ordinary double points [25]. It is also shown in [43] that a cubic surface possessing three ordinary double points can have, at most, 12 lines, which is the case for these eight cubic surfaces. Of these 12 lines on each surface, six are complex and six are real. Of the six real lines three are at infinity. The remaining three lines on each surface intersect each other in an equilateral triangle.

Different pairs of the eight cubic surfaces have one finite line in common, meaning there are 12 distinct finite lines among the eight surfaces. The finite lines contain the twelve edges of another stellated octahedron. The faces of the same stellated octahedron

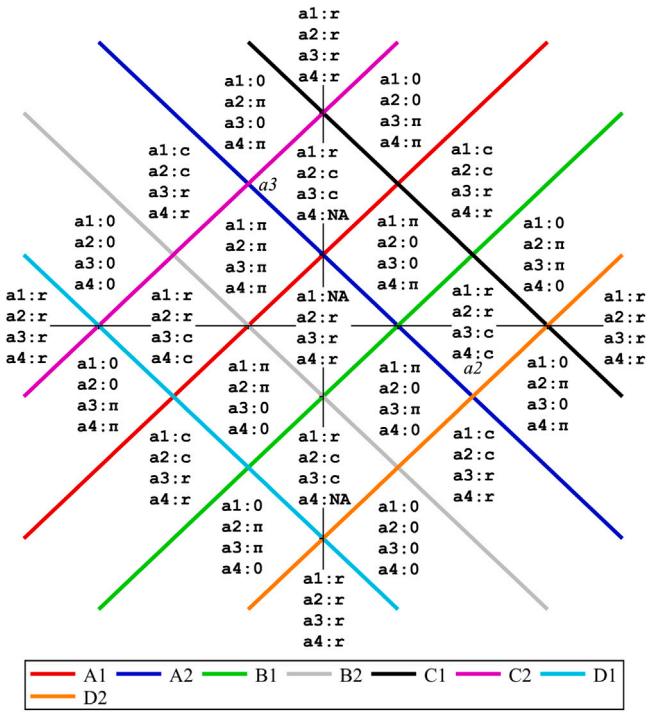

Fig. 7. Intersection of the planar 4R stellated octahedron in the design parameter space with the plane $a_1 = 0.5$.

are also found in the design parameter space of planar 4R linkages. The edges of this regular double tetrahedron can be regarded as the intersection of the bilinear factors of the coefficients of the planar 4R and the singular cubic surfaces formed by the coefficients of the spherical 4R IO equations in the design parameter spaces. This is as remarkable as it is fascinating! Fig. 6 illustrates the eight cubic surfaces and the three finite lines on each. This illustrates the connection between Bricard's movable octahedra mentioned at the end of Section 3 and the intersection of the spherical 4R and planar 4R design parameter spaces.

With the six algebraic $v_i - v_j$ equations, and the previously identified mobility classification using double points and discriminants, it becomes evident that the planes containing the faces of the stellated octahedron contain even more mobility information than stated in [36], namely, information on the relative mobility of every link in the chain! In fact, the stellated octahedron face planes segment the design parameter space into distinct regions which each describes the relative mobility of a_1, a_2, a_3 and a_4. Since a complete analysis of the design parameter space would go well beyond the scope of this paper, we will limit the discussion herein to one short example as follows.

Consider the intersection traces of the bilinear factors in the parameter plane $a_1 = 0.5$ spanned by a_2 and a_3 in the design parameter space where a_2 and a_3 are the horizontal and vertical axes, respectively. Here the bilinear factors are parallel and orthogonal plane trace lines. Together with Tables 4–7, the mobility of all a_2 and a_3 of any length can now be identified, resulting in Fig. 7 where **r** indicates that the corresponding link is a rocker, **c** a crank, π a π-rocker, and **0** a 0-rocker, while NA indicates the linkage is not assemblable. This analysis can be conducted for every area separated by the bilinear factors in the design parameter space, resulting in a complete geometric mobility classification of planar four bar linkages which is directly linked to the six algebraic $v_i - v_j$ IO equations.

6. Conclusions

In this paper we have derived the six possible planar 4R, RRRP, PRRP, and spherical 4R algebraic IO equations that describe the relative input and output joint displacement parameters between different pairs of edges of planar and spherical quadrangles providing a catalogue of 24 IO equations. They were derived using Study's soma coordinates that represent the displacement space of all kinematic chains, and polynomial elimination methods to reveal the desired algebraic IO equations. We showed that these algebraic polynomials define design parameter spaces, where distinct points represent distinct four-bar linkages. The location of the point in that space determines the linkage mobility characteristics. We showed that evaluating the nature of the double points at infinity in each of the $v_i - v_j$ planes gives conditions on the relative mobility of each link in the kinematic chain.

Declaration of competing interest

The authors declare that they have no known competing financial interests or personal relationships that could have appeared to influence the work reported in this paper.

Data availability

No data was used for the research described in the article.

Acknowledgements

The authors acknowledge the financial support of the Natural Sciences and Engineering Research Council of Canada (NSERC).

References

[1] M. Ceccarelli (Ed.), Distinguished Figures in Mechanism and Machine Science, Their Contributions and Legacies Part 1, Springer, NY, U.S.A., 2007.
[2] R. Willis, Principles of Mechanism, second ed., Cambridge University Press, Cambridge, England, 1841.
[3] F. Freudenstein, Design of Four-Link Mechanisms (Ph.D. thesis), Columbia University, New York, NY, U.S.A, 1954.
[4] J. Denavit, R.S. Hartenberg, A kinematic notation for lower-pair mechanisms based on matrices, Trans. ASME J. Appl. Mech. 22 (2) (1955) 215–221.
[5] M. Savage, A.S. Hall, Unique descriptions of all spherical four-bar linkages, ASME J. Eng. Ind. 92 (3) (1970) 559–563.
[6] C.R. Barker, J. Lo, Classification of spherical four-bar mechanisms, in: Proceedings of the 1986 ASME Mechanisms Conference, Columbus, OH, USA, 1986.
[7] C.H. Chiang, Kinematics of Spherical Mechanisms, Krieger Publishing Company, Malabar, FL, U.S.A., 2000.
[8] S.S. Balli, S. Chand, Transmission angle in mechanisms (triangle in mech), Mech. Mach. Theory 37 (2) (2002) 175–195.
[9] H.-P. Schröcker, M. Husty, J.M. McCarthy, Kinematic mapping based evaluation of assembly modes for planar four-bar synthesis, ASME J. Mech. Des. 129 (9) (2007) 924–929.
[10] S. Deshpande, A. Purwar, A machine learning approach to kinematic synthesis of defect-free planar four-bar linkages, J. Comput. Inf. Sci. Eng. 17 (2) (2019).
[11] Q.J. Ge, A. Purwar, P. Zhao, S. Deshpande, A task-driven approach to unified synthesis of planar four-bar linkages using algebraic fitting of a pencil of g-manifolds, J. Comput. Inf. Sci. Eng. 17 (2) (2019).
[12] S. Moazami, H. Zargarzadeh, S. Palanki, Kinematics of spherical robots rolling over 3D terrains, Complexity 2019 (2019) http://dx.doi.org/10.1155/2019/7543969.
[13] J. Plücker, Über ein neues coordinatensystem, J. Reine Angew. Math. (Crelle's J.) 5 (1830) 1–36.
[14] J. Plücker, On a new geometry of space, Philos. Trans. R. Soc. Lond. 155 (1865) 725–791.
[15] F. Klein, Vergleichende betrachtungen über neuere geometrische Forschungen, Erlangen, Math. Ann. 43 (1872) 63–100, Reprinted in 1893.
[16] E. Study, Geometrie der Dynamen, Teubner Verlag, Leipzig, Germany, 1903.
[17] O. Bottema, B. Roth, Theoretical Kinematics, Dover Publications, Inc., New York, N.Y., 1990.
[18] M. Husty, An algorithm for solving the direct kinematics of general Stewart-Gough platforms, Mech. Mach. Theory 31 (4) (1996) 365–379.
[19] E.J.F. Primrose, Planar Algebraic Curves, MacMillan, New York, NY, U.S.A., 1955.
[20] F. Klein, Elementary Mathematics from an Advanced Standpoint: Geometry, Dover Publications, Inc., New York, NY, U.S.A., 1939.
[21] M.L. Husty, A. Karger, H. Sachs, W. Steinhilper, Kinematik und Robotik, Springer-Verlag, Berlin, Heidelberg, New York, 1997.
[22] D. Cox, J. Little, D. O'Shea, Ideals, Varieties, and Algorithms: An Introduction to Computational Algebraic Geometry and Commutative Algebra, second ed., Springer-Verlag, Berlin, Germany, 1997.
[23] M. Rotzoll, M.J.D. Hayes, M.L. Husty, M. Pfurner, A general method for determining algebraic input-output equations for planar and spherical 4R linkages, in: J. Lenarčič, B. Siciliano (Eds.), Advances in Robotic Kinematics 2020, Springer International Publishing, Cham, Switzerland, 2021, pp. 90–97, http://dx.doi.org/10.1007/978-3-030-50975-0_12.
[24] M. Rotzoll, M.J.D. Hayes, A general method for determining algebraic input-output equations for the slider-crank and the bennett linkage, in: S. Nokleby, P. Cardou (Eds.), 11th CCToMM Symposium on Mechanisms, Machines, and Mechatronics, Ontario Tech University, Oshawa, ON, Canada, 2021.
[25] M.J.D. Hayes, M. Rotzoll, C. Ingalls, M. Pfurner, Design parameter space of spherical four-bar linkages, in: D. Pisla, B. Corves, C. Vaida (Eds.), New Trends in Mechanism and Machine Science, EuCoMeS, Springer Nature Switzerland AG.
[26] M. Pfurner, Analysis of Spatial Serial Manipulators Using Kinematic Mapping (Ph.D. thesis), University of Innsbruck, Innsbruck, Austria, 2006.
[27] A. Shabani, J.M. Porta, F. Thomas, A branch-and-prune method to solve closure equations in dual quaternions, Mech. Mach. Theory 164 (2021) http://dx.doi.org/10.1016/j.mechmachtheory.2021.104424.
[28] W. Adams, P. Loustaunau, An Introduction to Gröbner Bases, in: Graduate Studies in Mathematics, vol. 3, American Mathematical Society, 1994.
[29] M.J.D. Hayes, M. Rotzoll, M.L. Husty, Design parameter space of planar four-bar linkages, in: T. Uhl (Ed.), Advances in Mechanism and Machine Science, Springer Nature, Cham, Switzerland, 2019, pp. 229–238.
[30] A. Harnak, Über die vielteiligkeit der ebenen algebraischen curven, Math. Ann. 10 (1876) 189–198.
[31] A. Nichol, M. Rotzoll, M.J.D. Hayes, Planar RRRP mechanism design parameter space, in: S. Nokleby, P. Cardou (Eds.), 11th CCToMM Symposium on Mechanisms, Machines, and Mechatronics, Ontario Tech University, Oshawa, ON, Canada, 2021.
[32] R.S. Hartenberg, J. Denavit, Kinematic Synthesis of Linkages, McGraw-Hill, Book Co., New York, NY, U.S.A., 1964.
[33] R. Bricard, Mémoire sur la théorie de l'octaèdre articulé, J. Math. Pures Appl. 3 (1897) 113–148.
[34] M.J.D. Hayes, M. Rotzoll, A. Iraei, A. Nichol, Q. Bucciol, Algebraic differential kinematics of planar 4R linkages, in: 20th International Conference on Advanced Robotics, ICAR 2021, Ljubljana, Slovenia, 2021.
[35] A.P. Murray, P.M. Larochelle, A classification scheme for planar $4R$, spherical $4R$, and spatial $RCCR$ linkages to facilitate computer animation, in: Proceedings of 1998 ASME Design Engineering Technical Conferences (DETC'98), Atlanta, Georgia, U.S.A., 1998.
[36] M.J.D. Hayes, M. Rotzoll, M.L. Husty, M. Pfurner, Design parameter space of planar four-bar linkages, in: Proceedings of the 15th IFToMM World Congress, 2019.
[37] R. Cipolla, P. Giblin, Visual Motion of Curves and Surfaces, Cambridge University Press, Cambridge, U.K., 2000.
[38] C.M. Gosselin, J. Angeles, Representation graphique de la region de mobilite des mecanismes plans et spheriques a barres articulees, Mech. Mach. Theory 22 (6) (1987) 557–562, http://dx.doi.org/10.1016/0094-114X(87)90050-4, URL https://www.sciencedirect.com/science/article/pii/0094114X87900504.
[39] C.M. Gosselin, J. Angeles, Mobility analysis of planar and spherical linkages, Comput. Mech. Eng. (1988).
[40] C.M. Gosselin, J. Angeles, Optimization of planar and spherical function generators as minimum-defect linkages, Mech. Mach. Theory 24 (4) (1989) 293–307.
[41] H.S.M. Coxeter, Regular Polytopes, third ed., Dover Publications, Inc., New York, NY, U.S.A., 1973.
[42] M. Rotzoll, Q. Bucciol, M. Hayes, Algebraic input-output angle equation derivation algorithm for the six distinct angle pairings in arbitrary planar 4R linkages, in: 20th International Conference on Advanced Robotics, ICAR 2021, Ljubljana, Slovenia, 2021.
[43] B. Segre, The Non-Singular Cubic Surfaces; A New Method of Investigation with Special Reference to Questions of Reality, The Clarendon Press, Oxford, 1942.